Impact of seawater [Ca^{2+}] on the calcification and calcite Mg/Ca of *Amphistegina lessonii*

Antje Mewes[a]*, Gerald Langer[b], Silke Thoms[a], Gernot Nehrke[a], Gert-Jan Reichart[c,d], Lennart Jan de Nooijer[c], Jelle Bijma[a]

a: Alfred Wegener Institute Helmholtz Centre for Polar and Marine Research, Am Handelshafen 12, D-27570 Bremerhaven, Germany

b: Department of Earth Sciences, Cambridge University, Downing St., Cambridge, CB2 3EQ, UK

c: Royal Netherlands Institute for Sea Research, Landsdiep 4, 1797 SZ 't Horntje, Texel, The Netherlands

d: Department of Earth Sciences, Utrecht University, Budapestlaan, 4, 3584 CD Utrecht, The Netherlands

(*correspondence to: antje.mewes@awi.de; phone: +49 (0)471 4831 2291)

Keywords: Mg/Ca; proxy; LA-ICP-MS; culture experiment; biomineralization; *Amphistegina lessonii*

Abstract

Mg/Ca ratios in foraminiferal tests are routinely used as paleo temperature proxy, but on long timescales, also hold the potential to reconstruct past seawater Mg/Ca. Impact of both temperature and seawater Mg/Ca on Mg incorporation in foraminifera have been quantified by a number of studies. The underlying mechanism responsible for Mg incorporation in foraminiferal calcite and its sensitivity to environmental conditions, however, is not fully identified. A recently published biomineralization model (Nehrke et al., 2013) proposes a combination of transmembrane transport and seawater leakage or vacuolization to link calcite Mg/Ca to seawater Mg/Ca and explains inter-species variability in Mg/Ca ratios. To test the assumptions of this model, we conducted a culture study in which seawater Mg/Ca was manipulated by varying $[Ca^{2+}]$ and keeping $[Mg^{2+}]$ constant. Foraminiferal growth rates, test thickness and calcite Mg/Ca of newly formed chambers were analyzed. Results showed optimum growth rates and test thickness at Mg/Ca closest to that of ambient seawater. Calcite Mg/Ca is positively correlated to seawater Mg/Ca, indicating that not absolute seawater $[Ca^{2+}]$ and $[Mg^{2+}]$, but their ratio controls Mg/Ca in tests. These results demonstrate that the calcification process cannot be based only on seawater vacuolization, supporting the mixing model proposed by Nehrke et al. (2013). Here we, however, suggest a transmembrane transport fractionation that is not as strong as suggested by Nehrke et al. (20013).

Introduction

Foraminiferal test Mg/Ca_{CC} is a proxy used in paleoceanography to reconstruct past seawater temperatures (e.g. Nürnberg et al., 1996; Lear et al., 2000). In addition to temperature, calcite Mg/Ca_{CC} is also controlled by seawater Mg/Ca_{SW} (Segev and Erez, 2006; Evans and Müller, 2012). Since Mg/Ca_{SW} varied over geological time due to changes in the balance between Mg and Ca input and output, paleoceanographers need to account for this ratio in seawater, when using foraminiferal Mg/Ca_{CC} to reconstruct temperatures on timescales beyond ~ 1 Ma. Due to the long residence times of Mg^{2+} (~13 Ma) and Ca^{2+} (~1 Ma), this ratio does not need to be corrected for when using foraminiferal Mg/Ca on shorter timescales (Broecker and Yu, 2011; Hardie, 1996).

Biological processes involved in calcification complicate the relationships between Mg/Ca_{CC}, temperature and Mg/Ca_{SW}, which is apparent from large inter-species differences in Mg/Ca (Bentov and Erez, 2006). To improve the reliability of proxy relationships it is hence necessary to understand the impact of cellular processes involved in calcification. Controlled culture studies allow disentanglement of variables that often co-vary in the field, as well as allowing seawater conditions to be more extreme than naturally occurring. Studies by e.g. Erez (2003), and Bentov et al. (2009) suggested that foraminifers vacuolize seawater to acquire the ions needed for calcification. Seawater vacuolization would require the extraction of Ca^{2+} and CO_3^{2-} from the vacuoles or the removal of all unwanted ions, such as e.g. Mg^{2+}. However, studies by De Nooijer et al. (2009) and Nehrke et al. (2013) showed that the volume of vacuoles observed during calcification cannot account for the total amount of ions needed for calcification. An intracellular storage reservoir for inorganic carbon, or a "pool", was shown for the perforate foraminifer, *Amphistegina lobifera* (Ter Kuile et al. 1989), possibly corresponding to the

61 vacuoles described by Erez (2003) (De Nooijer et al. 2014). However, Ca^{2+} pools are absent in
62 the benthic *Ammonia aomoriensis*, demonstrated by Nehrke et al. (2013). On the basis of their
63 experiments these authors suggested that selective transmembrane transport (TMT) is responsible
64 for the delivery of Ca^{2+} to the site of calcification during chamber formation. A minor portion of
65 unfractionated elements may reach the site of calcification passively via seawater leakage or via
66 seawater vacuolization (Nehrke et al., 2013). This model predicts a linear relationship between
67 Mg/Ca_{SW} and Mg/Ca_{CC}, as observed for e.g. *Amphistegina lessonii* (Segev and Erez 2006, Mewes
68 et al. 2014), *Amphistegina lobifera* (Segev and Erez 2006) and *Ammonia aomoriensis* (Mewes et
69 al. 2014). In the experiments by Mewes et al. (2014), [Ca] was kept constant while [Mg] was
70 varied. To verify the TMT/PT model, requires investigating the effect of varying seawater [Ca]
71 on Mg/Ca_{CC}.

72 The aim of this culture study is to investigate the effect of different Mg/Ca_{SW} by varying
73 seawater [Ca] and keeping [Mg] constant, on test growth, test wall thickness and Mg/Ca_{CC}. The
74 results allow testing the assumptions of the calcification model by Nehrke et al. (2013) and are
75 used to construct a refined model.

76

2. Materials and Methods

2.1 Sampling and Storage of Specimens

The benthic foraminifer *Amphistegina lessonii* was chosen for this experiment because our experience has shown that *A. lessonii* grow and reproduce well in our laboratory. Due to its relatively large size of >1mm it is furthermore relatively easy to observe and handle. Because of cost efficient and easy accessibility coral l reef rubble with attached benthic foraminifera was sampled in April 2012 from a coral reef aquarium at Burger's Zoo, Arnhem, The Netherlands (Ernst et al., 2011). Sampling foraminifers from the zoo aquarium instead of the natural environment seems at first view not ideal. The zoo's aquarium is however one of the largest aquaria in the world, harboring a very rich (micro)fauna and providing spatially diverse microhabitats. In the present study we are dealing with a fairly fundamental aspect of physiology, namely with the response to concentrations and ratios of major ions in seawater. Zoo-specimens have no opportunity to adjust their physiological machinery to changing Mg and Ca, since these concentrations are the same in the aquarium as in the field. Upon return to the laboratory, samples were kept in an aquarium (AQUAEL 10), containing a heating element, light source (light intensity ~80 µmol/m^2s) and a small water pump with filter to circulate the water. For the experiments, specimens of *Amphistegina lessonii* were collected from the rubble using a small brush (section 2.3).

2.2 Preparation of Culture Media

From our experience with previous culture experiments we knew that some species of foraminifera do not grow well in 100% artificial seawater (ASW). A small pilot experiment, in

which we cultured *Amphistegina lessonii* in different mixtures of artificial (ASW) and natural seawater (NSW), revealed that a mixture of 30% NSW and 70% ASW results in optimal foraminiferal growth rates. To prepare culture media with constant [Mg], but varying [Ca], elemental concentrations of the available NSW were determined. Based on this, the concentrations to be added to the ASW (based on the recipe by Kester et al. (1967)) were calculated. Six different treatments with constant [Mg] (50mM) and varying [Ca] (3, 5, 7, 10, 21, 38 mM) were prepared, resulting in media with Mg/Ca ratios of ~16.6, 10, 7.1, 5, 2.4 and 1.5. Actual concentrations in the final culture media were verified by inductively coupled plasma - optical emission spectrometry (ICP-OES) and are summarized in table 1. Since salinity varied, depending on the varying [Ca], salinity was measured for all treatments (salinometer: WTW, Cond 330) and adjusted to a constant value (S=32.4), by adding NaCl from a stock solution (5 M). pH was measured using a pH meter (WTW, pH 3110, NBS scale) and adjusted to a constant value (pH=8.01) by adding 1M NaOH. Total alkalinity (TA) and dissolved inorganic carbon (DIC) were determined using a SI-Analytics TW alpha plus and a XY-2 Sampler, Bran und Luebbe, respectively. All values are summarized in table 1.

2.3 Juvenile *Amphistegina lessonii*

For the culture experiment we used in culture grown offspring of the zoo-derived specimens. For the culture experiment we used in culture grown offspring of the zoo-derived specimens. Offspring were used to ensure that most of their calcite is formed during incubation in controlled conditions. To obtain juveniles, adult specimens were picked from the stock material. Adult specimens crawled up the aquarium glass walls, facilitating selection of living specimens, and transfered to well plates. Well plates were placed in light (12h light / 12h dark cycle) and

temperature controlled incubators (RUMED, Rubarth Apparate GmbH) at 25°C. The daylight sources had a light intensity of 130 µmol/m^2/s at the level of the well plates. After a few days, about 10% of the specimens had reproduced asexually. These juveniles were selected for the culturing experiments and evenly distributed between the different treatments.

2.4 Culture Experiment

The culture protocol was the same as reported in Mewes et al. (2014), except for the manipulation of the culture media (compare 2.2). Juveniles of *A. lessonii* were incubated in petri dishes, containing ~10 ml of culturing medium. In total, juveniles of 4 different broods were used and divided equally over the treatments (each brood in duplicates containing 5-10 individuals per petri dish), resulting in 50 to 56 juveniles for every treatment. To maintain constant culture conditions, the culture media was replaced once every three days. Immediately after replacement of the media, specimens were fed 100 µl of a dense culture of the green algae *Dunaliella salina* (~$4*10^6$ cells*mL^{-1}). To prevent bacterial colonialization of petri dishes due to left-over food, all All specimens were transferred to a clean petri dish once every week. This resulted in an occasional loss of some specimens. Dead specimens were identified by a change in color from brownish/greenish to pale/white, due to their loss of symbionts. Survival rates were high (ca. 95%) and not correlated with any measured parameter. Dead specimens were removed from culture. The culture experiment ran for ~7 weeks and resulted in a final number of successfully grown juveniles between 37 and 56 per treatment.

Alkalinity was determined once every week and culture media element concentrations were measured a second time at the end of the experiment. Prior to analyses media were filtered (syringe filter 0.2 µm).

2.3. Determination of size and growth rates

The maximum test size [µm] of all specimens was measured weekly using a digital camera (AxioCam MRc5) connected to a Zeiss microscope (Axiovert 200M). Maximum test diameters were determined from pictures using the Axiovision (Zeiss) software. Foraminiferal test size increased with time and from the resulting regression, growth rates in [µm/day] were calculated. In foraminifera, biomass increases continuously, whereas chamber formation is intermittent (e.g. Signes et al., 1993). Because we did not observe the duration of actual chamber formation, reported rates refer to overall growth rates, which should not be confused with calcium carbonate precipitation rates.

2.4 Cleaning Procedure

After termination of the experiment, all specimens were rinsed with distilled water and placed in a 7% NaOCl solution for 4 hours to remove organic material. Specimens were rinsed again and dried overnight (12 h) in an oven at 60°C.

2.5 Determination of weight and size normalized weight

Test weight was determined with an ultra-microbalance (Mettler Toledo UMX2, precision: ± 0.1 µg). Due to the limited weight of individual specimens, each replicate group was weighed as a whole, resulting in n = 8 (duplicates x 4 broods) measurements. Mean weight per specimen was determined by dividing the weight of each replicate by the number of specimens in the group.

166 Weight was normalized to the final size measured with the microscope. This size normalized
167 weight (SNW) is an indication for test wall thickness and defined by:

168 $$SNW = \frac{weight\ [\mu g]}{size\ [\mu m]}$$

169 Size normalized weight also depends on the time spend in culture, which makes it challenging to
170 compare SNW measured in our experiment to other experiments. Thus, we expressed size
171 normalized weight as relative SNW [%], such that it is related to the highest SNW in each of the
172 experiments (which equals 100%).

173

174 **2.6 Element Measurements**

175 Elemental concentrations were determined using laser-ablation inductively coupled plasma mass
176 spectrometry (LA-ICP-MS). For this purpose, analyses were done on the GeoLas 22Q Excimer
177 laser (Lambda Physik), coupled to a sector field ICP-MS (Element 2, Thermo Scientific) at
178 Utrecht University (Reichart et al., 2003). Prior to analyses, specimens were mounted on stubs
179 with double-sided adhesive tape. Depending on the size of the chambers, laser spot size was set
180 to 80, 60 or 40 µm to ablate as much material as possible while at the same time avoiding
181 contamination from adjacent chambers. From each replicate group in each of the treatments, 4-6
182 chambers of one to two specimens were analyzed, resulting in 50 to 65 measurements per
183 treatment. Data from single chamber measurements were calibrated against a glass standard
184 (SRM NIST 610; Jochum et al. 2011). To assure high signal quality (e.g. to correct for drift),
185 every 10-15 measurements two NIST standards were measured. Laser repetition rate was set to 7
186 Hz and the energy density was set to ~1,2 J*cm^{-2} when ablating calcite and to ~5 J*cm^{-2} when
187 ablating glas. Elemental concentrations were calculated for ^{24}Mg, ^{26}Mg and ^{43}Ca, ^{44}Ca using

188 GLITTER (version 4.4.3). An in-house made carbonate standard with known Mg/Ca and Sr/Ca
189 (was measured at an energy density of ~1.2 J*cm^{-2} every 10-12 foraminiferal samples and
190 allowed to check for matrix effects that may result from switching between energy densities
191 (Dueñas-Bohórquez et al., 2009; 2011). All profiles were evaluated individually and parts of the
192 profiles, where ^{27}Al and/or ^{55}Mn (indicating potential contamination) was elevated, were rejected.
193 From a total of 305 ablations, 17 had to be discarded, either because of contamination, or due to
194 short ablation profiles, typically from the thinly calcified last chamber. Mg fractionation,
195 expressed as the partition coefficient for Mg (D_{Mg}), was calculated by dividing the Mg/Ca of the
196 calcite (Mg/Ca_{CC}) by the Mg/Ca of seawater (Mg/Ca_{SW}):

197 $$D_{Mg} = \frac{Mg/Ca_{CC}}{Mg/Ca_{SW}}$$

3. Results

3.1 Morphological Parameters

3.1.1 Size and Growth Rates

Figure 1a shows growth of foraminifers in the different treatments. At very low [Ca] (3 mM) foraminifers did not grow (Figure 1a). With increasing [Ca], growth rates progressively increased, whereas at highest seawater [Ca] (34 mM), growth rates were reduced again. At lower [Ca] (e.g. Ca = 5 mM and 7 mM), growth seemed to cease before termination of the experiment while in the treatments with higher [Ca] (e.g. Ca = 9 mM and 18 mM) growth continued throughout the experiment.

Figure 1b shows the final mean test size for the different treatments. Largest test size of 503 µm suggests that optimal growth conditions were attained at [Ca] = 17.9 mM and Mg/Ca_{SW} = 2.9, directly followed by the control treatment near ambient at [Ca] = 9 mM and Mg/Ca = 5.7 with a final test size of 428 µm (Figure 1b).

3.1.2 Size normalized weight

Figure 2 shows size normalized weight, a measure for test wall thickness, for the different treatments. Similar to growth, size normalized weights were also highest (0.21 µg/µm) at seawater [Ca] = 9 mM and Mg/Ca_{SW} = 5.7. Seawater [Ca] lower or higher than this condition resulted in reduced size normalized weight and hence test wall thicknesses.

3.2 Calcite Mg/Ca

Figure 3a shows the relationship between Mg/Ca_{CC} and Mg/Ca_{SW}. With increasing Mg/Ca_{SW} and thus decreasing seawater [Ca] (and decreasing Ω), Mg/Ca_{CC} increases. This relationship can be described by a linear regression with a positive y-intercept. The relationship between the distribution coefficient, D_{Mg}, and Mg/Ca_{SW}, is best described by an exponential decrease, approaching an asymptote (Figure 3b).

4. Discussion

4.1 Growth rates and size normalized weight

Growth rates [µm/d] varied substantially with seawater [Ca] (Figure 1). Except for the treatment with highest seawater [Ca], increased [Ca] levels correlate to increased growth rates. Considering only the current dataset by itself one could get to the conclusion that increasing [Ca] causes faster growth until a certain toxic level at [Ca] > 18 mM. However, comparing the present dataset with the one from Mewes et al. (2014), where the absolute [Mg] was varied and [Ca] was kept constant, shows that the calcium concentration by itself is not be the primary driver of growth rate but that it is controlled by the Mg/Ca of seawater. To compare data in the present study with those from Mewes et al. (2014), growth rates (in µm/day) were derived from a linear regression curve fitted to the size data of the first 30 days (Figure 4). It is not possible to derive growth rates from a linear regression line fitted to the time span of the whole experiment (49 days), due to the saturation of growth in the present study after 30 days (Figure 1a). As a result, the time spans of growth between the two culture studies are different and do not allow a simple comparison of final test size.

Mewes et al. (2014) varied seawater [Mg] and kept [Ca] constant at 10 mM, observing a similar optimum at ambient Mg/Ca_{SW}. An increase of seawater [Mg] from ~50 mM to ~ 90 mM decreased growth rates even more than lowering of [Mg] from ~50 mM to ~14 mM. The varying growth rates in the Mewes et al. (2014) dataset, at constant [Ca] clearly show that not the calcium concentration itself is the primary driver of growth rates. Considering both datasets rather suggest that seawater Mg/Ca_{SW} ratio is the primary driver of growth rates and not the absolute concentrations of Ca or Mg. Apparently, the optimum Mg/Ca_{SW} for foraminiferal growth is between 3 and 5 mol/mol (Figure 4). In a similar study, Segev and Erez (2006) measured growth

249 rates in *Amphistegina* spp. as a function of seawater Mg/Ca in terms of $CaCO_3$ addition, similarly
250 concluding that the Mg/Ca ratio of seawater is the main driver of the specimens' growth rates.
251 Their data suggest that highest growth rate is reached at Mg/Ca_{SW} of ~1, while a ratio of ~0.5 was
252 suboptimal. Because Mg is known to inhibit inorganic calcite precipitation, they concluded that
253 *Amphistegina spp.* is able to precipitate its test more easily from seawater with lower Mg/Ca
254 ratios. While this argument is based on a comparison with the inorganic system, their explanation
255 for the decline in growth rate at Mg/Ca_{SW} ~ 0.5 mol/mol is based on physiology, i.e. that a
256 minimum of Mg is required for foraminiferal growth. This physiological explanation can in itself
257 not fully explain our results, because the lowest Mg/Ca_{SW} in our studies (the present one and
258 Mewes et al. 2014) was achieved through both elevating seawater [Ca] and lowering [Mg].
259 Interestingly, growth rates at lowest Mg/Ca_{SW}, is lower in the case of the Ca-variable experiment,
260 indicating that at this particular Mg/Ca the high Ca concentration may be more detrimental to
261 growth than the low Mg concentration (Figure 4). The latter observation can neither be explained
262 in terms of inorganic calcite precipitation nor in terms of a minimum Mg requirement. However,
263 it may be that high seawater [Ca] may be toxic for the cell (e.g. Martinez-Colon et al., 2009).
264 Together, the results of Segev and Erez (2006) and those presented here strongly suggest that
265 growth in *Amphistegina spp.* is influenced by the Mg/Ca_{SW} ratio. With these datasets, it is
266 currently impossible to determine the optimal Mg/Ca_{SW} ratio for foraminiferal growth, because
267 the available datasets suggest a plateau, rather than a clearly defined peak-value. Our dataset (Fig.
268 4) suggests an optimum between 3 and 5 mol/mol, but may range from 2 to 5 mol/mol. The
269 dataset of Segev and Erez (2006) locates the optimum between 1 and 2.5 mol/mol. But this is a
270 potentially biased range, because there are no data between Mg/Ca_{SW} of 2.5 and 5 mol/mol. This
271 implies that these two datasets combined (Fig. 4, Segev and Erez 2006) suggest an optimum
272 between 1 and 5 mol/mol. While this might appear to be a large range, it is a reasonable interval

from a physiological perspective, because physiological optima usually comprise a range of values. Well known examples are temperature, light intensity, and nutrient concentrations. The same argumentation also applies to SNW (figure 5). This is the first study showing the effect of Mg/Ca_{SW} on foraminiferal SNW. The effect of Mg/Ca_{SW} on foraminiferal SNW shows the same trend (optimum curve) as the effect of Mg/Ca_{SW} on growth rates. Similar trends for growth rate and SNW in response to seawater carbonate chemistry changes were described for another benthic foraminifer, namely *Ammonia tepida* (i.e. *A. aomoriensis*) (Keul et al., 2013). It should be emphasized that comparison of absolute values for SNW or growth rate between different experiments is challenging since observed values are highly variable, even under similar culture conditions. This is not confined to foraminifers, but also known from culture studies using coccolithohores (Hoppe et al., 2011). It is therefore reasonable to follow the recommendation of Hoppe et al. (2011) and base interpretations on response patterns, i.e. trends, rather than absolute values.

4.2 Calcite Mg/Ca

Our results show that Mg/Ca_{CC} increases linearly with decreasing seawater [Ca] and thus increasing Mg/Ca_{SW} (Figure 3a). Comparison to our previous study, where [Mg] was varied and [Ca] was kept constant (Mewes et al., 2014) shows a strong agreement between the two data sets (Figure 6a). This suggests that test Mg/Ca_{CC} is controlled by the ratio of Mg to Ca in seawater, rather than by absolute concentrations. This result would be in accordance with a calcification mechanism based on seawater vacuolization, if the Mg transport mechanism features a Ca fractionation independent of seawater Mg or Ca concentrations. While this is a perfectly reasonable scenario, it makes little sense when considering the assumed function of this transport,

296 i.e. Mg homoeostasis. In other words, if the behavior of the Mg transporter is compatible with our
297 data, it cannot perform its alleged role. Calcification based on vacuolization might exclude Mg
298 homoeostasis as a function of this transporter and instead, the function might merely be a
299 lowering of the Mg/Ca ratio. Hence the question whether our data are compatible with a
300 calcification mechanism based on vacuolization of seawater, depends on the precise
301 interpretation of this mechanism.

302 Foraminiferal Mg/Ca_{CC} at varying Mg/Ca_{SW} can be used to test the biomineralization
303 model developed by Nehrke et al. (2013). This model assumes that foraminifers obtain the
304 majority of Ca^{2+}, needed for calcification, via highly selective transmembrane transport (TMT)
305 and that the majority of the Mg^{2+} stems from (unfractionated) seawater leakage or vacuolar
306 transport (i.e "passive transport (PT)). In contrast to the vacuole-based biomineralization model
307 (e.g. Bentov and Erez 2006, Bentov et al. 2009), the TMT/PT mixing model assumes that the
308 percentage of ions transported via PT, is very small compared to those delivered by TMT. Given
309 that elements are not fractionated during the transport of vacuoles to the site of calcification,
310 contribution from vacuole-bound ions or seawater leakage plays a key role in determining the
311 Mg/Ca_{CC}. The model explains the difference between low, medium and high-Mg calcite species
312 via an increasing relative contribution of PT. As already suggested by Nehrke et al. (2013), the
313 model predictions can be tested with culture studies such as this one.

314 The mixing model (Nehrke et al., 2013) predicts a linear relationship between Mg/Ca_{CC}
315 and Mg/Ca_{SW}, intersecting with the origin. As discussed by Mewes et al. (2014), the relationship
316 between Mg/Ca_{CC} and Mg/Ca_{SW} is best described by a linear relationship having a positive
317 intercept (figure 6a). At high Mg/Ca_{SW} this relationship is in line with the mixing model (Nehrke
318 et al. 2013). At very low Mg/Ca_{SW}, however, the present and our previous data have a positive y-

intercept, i.e. an increased D_{Mg} (Figure 6b), which is not predicted by the model of Nehrke et al. (2013) (for discussion see Mewes et al. (2014)). Here we present a refined flux-based model, which solves this problem (for the mathematical derivation see Appendix). The model is based on the same assumptions as Nehrke et al. (2013): the total ion flux is divided into passive transport (PT) and transmembrane transport (TMT) (mixing model). The fraction of the total flux of the divalent cations transported via PT, is expressed as *x* (see equation A2). Similar to Nehrke et al. (2013), we assume no fractionation during passive transport, while we assume a strong fractionation (*frac*) during TMT (see equations A4 and A5). The Mg/Ca_{CC} ratio of the precipitated calcite represents the Mg/Ca ratio of the two different fluxes (see equation A10). A further fundamental assumption is that Mg^{2+} substitutes for Ca^{2+} in the calcite lattice, i.e. in a given volume of calcite the sum of Mg and Ca ions is constant. Based on data showing high Mg areas in conjunction with organic layers in the shell, it was traditionally assumed that Mg^{2+} may be incorporated in the organic layers, rather than in the calcite lattice alone (Erez 2003). However, by means of nano-scale synchrotron X-ray spectroscopy, Branson et al. (2013) showed that most of the Mg present in foraminiferal shells substitutes for Ca in the calcite lattice. Therefore the assumption that the sum of Mg and Ca is constant is justified.

Based on the above assumptions the refined flux-based model yields calcite Mg/Ca

$$\left(\frac{Mg^{2+}}{Ca^{2+}}\right)_{CC} = R_{SW}\left[\frac{frac(1-x)+x+frac\cdot R_{SW}}{1+(1-x+frac\cdot x)R_{SW}}\right]$$

The curve (figure 7a) can be fitted over the whole R_{SW} (= Mg/Ca_{SW}) with a TMT fractionation frac = 0.005 and a contribution of PT to the total ion flux x = 0.02. The TMT fractionation, i.e. 0.005 (=frac) is weaker than the one assumed in the previous model (0.0001; Nehrke et al., 2013). This is a reasonable modification because Mg TMT fractionation is not known in either

coccolithophores or foraminifera and typical Ca channels display a range of Mg fractionation (e.g. White, 2000).

The partition coefficient for Mg is given by:

$$D_{Mg^{2+}} = \left(\frac{Mg^{2+}}{Ca^{2+}} \right)_{CC} \Big/ R_{SW} = \frac{frac(1-x) + x + frac \cdot R_{SW}}{1 + (1 - x + frac \cdot x) R_{SW}}$$

This refined flux-based model predicts both the trend of Mg/Ca_{CC} versus Mg/Ca_{SW} and D_{Mg} versus Mg/Ca_{SW}. Especially the dependence of D_{Mg} on Mg/Ca_{SW} is interesting because the trend observed here (figure. 6b and 7b) was also reported for inorganically precipitated calcite (Mucci and Morse 1983). Segev and Erez (2006) already noted that curious fact. They commented: “A physiological mechanism sensitive to ratio ... remains to be explored” (Segev and Erez 2006). We present such a physiological mechanism, which comprises transmembrane transport and seawater vacuolization. Our refined flux-based model for major and minor element incorporation therefore represents a promising new way of interpreting foraminiferal element to calcium ratios. Future research should hence be concerned with the question whether the behavior of other elements can be reconciled with our model.

5. Summary

Our study showed optimum growth performance of *Amphistegina lessonii* at Mg/Ca_{SW} near ambient. Growth rates, test wall thickness and also test Mg/Ca_{CC} is not controlled by absolute seawater [Ca] and [Mg], but by their ratio in seawater. We provide further support for the recently developed biomineralization model by Nehrke et al. (2013) and present a refined flux-based model which predicts our experimentally determined dependence of Mg/Ca_{CC} on Mg/Ca_{SW}.

Appendix: refined TMT+PT mixing model

The transport of Mg^{2+} and Ca^{2+} in our flux-based model is described in terms of the total flux of the bivalent cations

$$F_{CAT} = F_{Ca^{2+}} + F_{Mg^{2+}} \quad . \tag{A1}$$

The total ion flux is sub-divided into passive transport (PT) and transmembrane transport (TMT). Assuming that a fraction x of the total flux is transported via PT, the fluxes of bivalent cations for both transport pathways are expressed as

$$F_{PT} = F_{PT,Ca^{2+}} + F_{PT,Mg^{2+}} = xF_{CAT} \tag{A2}$$

$$F_{TMT} = F_{TMT,Ca^{2+}} + F_{TMT,Mg^{2+}} = (1-x)F_{CAT} \tag{A3}$$

The contribution of Ca^{2+} and Mg^{2+} to PT and TMP is controlled by the fractionation during transport. It is assumed that no fractionation takes place during passive transport, but a strong fractionation (*frac*) during TMT. Based on this assumption the ratios of Ca^{2+} and Mg^{2+} fluxes are given by

$$\frac{F_{PT,Mg^{2+}}}{F_{PT,Ca^{2+}}} = R_{SW}\,, \tag{A4}$$

$$\frac{F_{TMT,Mg^{2+}}}{F_{TMT,Ca^{2+}}} = frac \cdot R_{SW}\,, \tag{A5}$$

where R_{SW} is the seawater Mg/Ca. Combination of equations (A2)-(A5) yields the Ca^{2+} and Mg^{2+} fluxes for the PT and TMT pathways

$$F_{PT,Mg^{2+}} = \frac{R_{SW}}{1+R_{SW}} x \cdot F_{CAT}\,, \tag{A6}$$

$$F_{PT,Ca^{2+}} = \frac{1}{1+R_{SW}} x \cdot F_{CAT}\,, \tag{A7}$$

$$F_{TMT,Mg^{2+}} = \frac{frac \cdot R_{SW}}{1+\ frac \cdot R_{SW}} (1-x) F_{CAT}\,, \tag{A8}$$

$$F_{TMT,Ca^{2+}} = \frac{1}{1+\ frac \cdot R_{SW}} (1-x) F_{CAT}\,. \tag{A9}$$

The Mg/Ca_{CC} ratio of the precipitated calcite represents the Mg/Ca ratio of the ion fluxes:

$$\left(\frac{Mg^{2+}}{Ca^{2+}}\right)_{CC} = \frac{F_{TMT,Mg^{2+}} + F_{PT,Mg^{2+}}}{F_{TMT,Ca^{2+}} + F_{PT,Ca^{2+}}} = \frac{\frac{frac \cdot R_{SW}}{1+\ frac \cdot R_{SW}} (1-x) F_{CAT} + \frac{R_{SW}}{1+R_{SW}} x \cdot F_{CAT}}{\frac{1}{1+\ frac \cdot R_{SW}} (1-x) F_{CAT} + \frac{1}{1+R_{SW}} x \cdot F_{CAT}}\,, \tag{A10}$$

which can be written as:

$$\left(\frac{Mg^{2+}}{Ca^{2+}}\right)_{CC} = R_{SW}\left[\frac{frac(1-x)+x+\ frac \cdot R_{SW}}{1+(1-x+\ frac \cdot x)R_{SW}}\right]. \tag{A11}$$

Equation (A11) indicates that the calcite Mg/Ca depends on the seawater Mg/Ca, but not on the total flux of the bivalent cations (F_{CAT}). This explains why test Mg/Ca is controlled by the ratio of Mg and Ca, but not by their absolute concentrations in seawater. The partition coefficient for Mg (D_{Mg2+}) is defined with respect to seawater Mg/Ca, thus

$$D_{Mg^{2+}} = \left(\frac{Mg^{2+}}{Ca^{2+}}\right)_{CC} \Big/ R_{SW} = \frac{frac(1-x)+x+\ frac \cdot R_{SW}}{1+(1-x+\ frac \cdot x)R_{SW}}\,. \tag{A12}$$

References

Branson, O., Redfern, S. A., Tyliszczak, T., Sadekov, A., Langer, G., Kimoto, K., and Elderfield, H.: The coordination of Mg in foraminiferal calcite, Earth and Planetary Science Letters 383, 134-141, 2013.

Broecker, W.,Yu, J.: What do we know about the evolution of Mg to Ca ratios in seawater?, Paleoceanography 26, PA3203, 2006.

Bentov, S. and Erez, J.: Impact of biomineralization processes on the Mg content of foraminiferal shells: A biological perspective, Geochemistry Geophysics Geosystems 7, 1-11, 2006.

Bentov, S., Brownlee, C. and Erez, J.: The role of seawater endocytosis in the biomineralization process in calcareous foraminifera, Proceedings of the National Academy of Sciences 106, 21500-21504, 2009.

De Nooijer, L. J., Langer, G., Nehrke, G., and Bijma, J.: Physiological controls on seawater uptake and calcification in the benthic foraminifer *Ammonia tepida*, Biogeosciences, 6, 2669-2675, 2009.

Dueñas-Bohórquez, A., da Rocha, R. E., Kuroyanagi, A., Bijma, J., Reichart, G. J.: Effect of salinity and seawater calcite saturation state on Mg and Sr incorporation in cultured planktonic foraminifera, Marine Micropaleontology, 73(3), 178-189, 2009.

Dueñas-Bohórquez, A., Da Rocha, R. E., Kuroyanagi, A., De Nooijer, L. J., Bijma, J., Reichart, G. J.: Interindividual variability and ontogenetic effects on Mg and Sr incorporation in the planktonic foraminifer *Globigerinoides sacculifer*, Geochimica et Cosmochimica Acta, 75(2), 520-532, 2011.

Erez, J: The Source of Ions for Biomineralization in Foraminifera and Their Implications for Paleoceanographic Proxies, Reviews in Mineralogy and Geochemistry 54, 115-149, 2003.

Ernst, S., Janse, M., Renema, W., Kouwenhoven, T., Goudeau, M. L., & Reichart, G. J.: Benthic foraminifera in a large Indo-Pacific coral reef aquarium, The Journal of Foraminiferal Research, 41(2), 101-113, 2011.

Evans, D., & Müller, W.: Deep time foraminifera Mg/Ca paleothermometry: Nonlinear correction for secular change in seawater Mg/Ca, Paleoceanography, 27(4), 2012.

Glas, M. S., Langer, G., and Keul, N.: Calcification acidifies the microenvironment of a benthic foraminifer (*Ammonia sp.*), Journal of Experimental Marine Biology and Ecology, 424, 53-58, 2012.

Hardie, L.A.: Secular variation in seawater chemistry: An explanation for the coupled secular variation in the mineralogies of marine limestones and potash evaporites over the past 600 my, Geology 24, 279-283, 1996.

Hoppe, C. J. M., Langer, G. and Rost, B.: *Emiliania huxleyi* shows identical responses to elevated pCO_2 in TA and DIC manipulations, Journal of Experimental Marine Biology and Ecology, 406, 54-62, 2011.

Jochum, K.P., Weis, U., Stoll, B., Kuzmin, D., Yang, Q.C., Raczek, I., Jacob, D.E., Stracke, A., Birbaum, K., Frick, D.A., Gunther, D. and Enzweiler, J.: Determination of reference values for NIST SRM 610-617 glasses following ISO guidelines, Geostandards and Geoanalytical Research 35, 397-429, 2011.

Kester, D.R., Duedall, I.W., Connors, D.N. and Pytkowicz, R.M.: Preparation of artificial seawater, Limnology and Oceanography 12, 176-179, 1967.

Keul, N., Langer, G., de Nooijer, L. J. and Bijma, J.: Effect of ocean acidification on the benthic foraminifera *Ammonia sp.* is caused by a decrease in carbonate ion concentration, *Biogeosciences, 10*, 6185-6198, 2013.

Lear, C. H., Elderfield, H., & Wilson, P. A.: Cenozoic deep-sea temperatures and global ice volumes from Mg/Ca in benthic foraminiferal calcite, Science, 287(5451), 269-272, 2000.

Lee, A. and East, J.: What the structure of a calcium pump tells us about its mechanism, Biochemical Journal, 356, 665-683, 2001.

Martínez-Colón, M., Hallock, P. and Green-Ruíz, C.: Strategies for using shallow-water benthic foraminifers as bioindicators of potentially toxic elements: a review, The Journal of Foraminiferal Research, 39, 278-299, 2009.

Mewes, A., Langer, G., de Nooijer, L.J., Bijma, J. and Reichart, J.G.: Effect of different seawater Mg^{2+} concentrations on calcification in two benthic foraminifers, Marine Micropaleontology, 2014.

Mucci, A. and Morse, J. W.: The incorporation of Mg^{2+} and Sr^{2+} into calcite overgrowths: influences of growth rate and solution composition, Geochimica et Cosmochimica Acta, 47(2), 217-233, 1983.

Nehrke, G., Keul, N., Langer, G., de Nooijer, L. J., Bijma, J., and Meibom, A.: A new model for biomineralization and trace-element signatures of foraminifera tests, Biogeosciences 10, 6759-6767, 2013.

Nelson D. L. and M. M. Cox: Lehninger Principles of Biochemistry, W. H. Freeman, 6th revised international edition 2013

Nürnberg, D., Bijma, J., & Hemleben, C.: Assessing the reliability of magnesium in foraminiferal calcite as a proxy for water mass temperatures, Geochimica et Cosmochimica Acta, 60(5), 803-814, 1996.

Raitzsch, M., Dueñas-Bohórquez, A., Reichart, G. J., de Nooijer, L. J., and Bickert, T.: Incorporation of Mg and Sr in calcite of cultured benthic foraminifera: impact of calcium concentration and associated calcite saturation state, Biogeosciences, 7(3), 869-881, 2010.

Segev, E. and Erez, J.: Effect of Mg/Ca ratio in seawater on shell composition in shallow benthic foraminifera, Geochemistry Geophysics Geosystems 7 (2), 1-8, 2006.

Spero, H. J.: Ultrastructural examination of chamber morphogenesis and biomineralization in the planktonic foraminifer *Orbulina universa*, Marine Biology, 99, 9-20, 1988.

Signes, M., Bijma, J., Hemleben, C., and Ott, R.: A model for planktic foraminiferal shell growth, Paleobiology, 71-91, 1993.

Ter Kuile, B., Erez, J. and Padan, E.: Mechanisms for the uptake of inorganic carbon by two species of symbiont-bearing foraminifera, Marine Biology, 103(2), 241-251, 1989.

White, P. J.: Calcium channels in higher plants, Biochimica et Biophysica Acta (BBA) - Biomembranes, 1465(1), 171-189, 2000.

Acknowledgement

Max Janse and his team are acknowledged for providing specimens from a coral reef tank at Burger's Zoo, in Arnhem, The Netherlands. Laura Wischnewski is acknowledged for her assistance with culturing foraminifers. We furthermore like to thank the technical assistance of Ulrike Richter, who prepared algae cultures, Jana Hölscher for doing DIC measurements, Ilsetraut Stölting for doing ICP-OES analyses and Helen de Waard for assisting during LA-ICP-MS analyzes at Utrecht University. This work was funded in part by The European Research Council (ERC grant 2010-NEWLOG ADG-267931 HE).

Tables

Table 1: Details of culture media as well as morphological and chemical test parameters

	Amphistegina lessonii					
	treat. 1	treat. 2	treat. 3	treat. 4	treat. 5	treat. 6
SW Mg^{2+} [mM]	51.64	52.56	52.75	52.66	52.05	52.40
SW Ca^{2+} [mM]	34.19	17.86	9.22	6.63	4.77	3.18
Mg/Ca_{SW} [mol/mol]	1.51	2.94	5.72	7.95	10.91	16.47
± st. error	±0.00	±0.03	± 0.02	± 0.05	± 0.07	± 0.09
Mg/Ca_{CC} [mmol/mol]	22.95	40.79	52.08	67.50	83.35	-
± st. error	±0.81	±1.38	±1.72	±2.37	±1.96	
T [°C]	25	25	25	25	25	25
S ‰	32.4	32.4	32.4	32.4	32.4	32.4
pH (NBS)	8.1	8.1	8.1	8.1	8.1	8.1
TA [µmol/kg]	2615	2545	2504	2504	2492	2479
Ω (calcite)	16.75	8.74	4.49	3.24	2.33	1.55
DIC [µmol/kg]	2302	2298	2286	2295	2294	2290
final test size [µm]	362.7	503.4	427.5	341.1	240.6	138.4
± st. error	±9.3	±9.1	±6.4	±5.9	±7.9	±7.8
growth rate [µm/day]	4.21	8.15	6.91	5.89	2.95	-0.53
± st. error	±0.36	±0.46	±0.84	±0.13	±0.91	±0.21
mean SNW*1000	124.64	190.90	206.22	163.34	78.94	24.60
[µg/µm] ± st. dev.	±26.13	±29.40	±23.61	±26.51	±40.56	±16.43

Figures and Figure captions

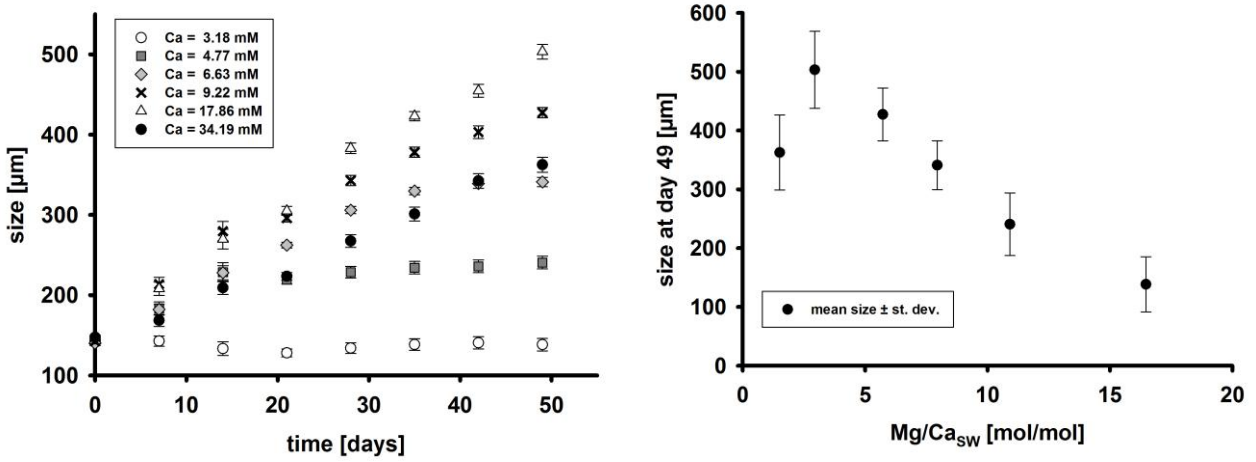

a) b)

Figure 1: a) Mean test size ± st. error for all treatments versus time in culture (n = 37-56). b) Mean test size ± st. dev. at the end of the experiment versus seawater Mg/Ca.

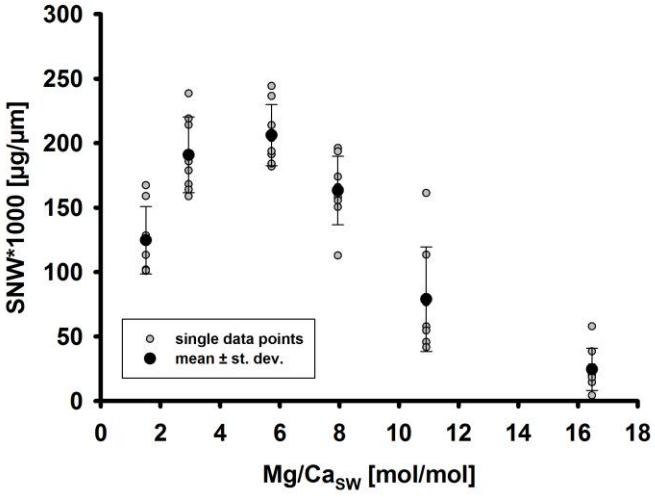

Figure 2: Size normalized weight versus seawater Mg/Ca (n = 8).

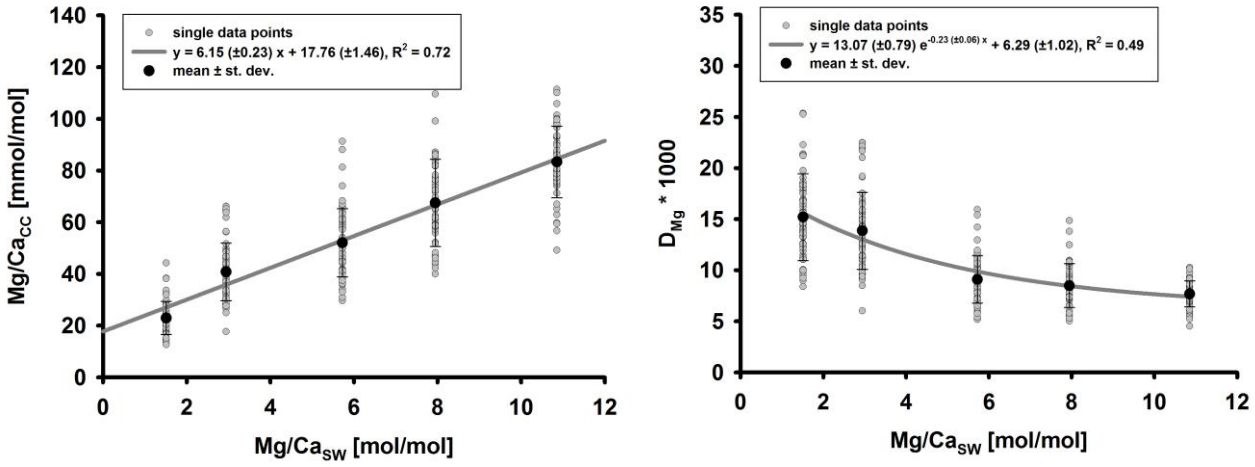

a) b)

494 Figure 3: a) Mg/Ca_{CC} versus Mg/Ca_{SW} ([Ca] and thus Ω decreases with increasing Mg/Ca_{SW}) and
495 b) D_{Mg} x 1000 versus Mg/Ca_{SW} (n=50-65 ablations per treatment).

496

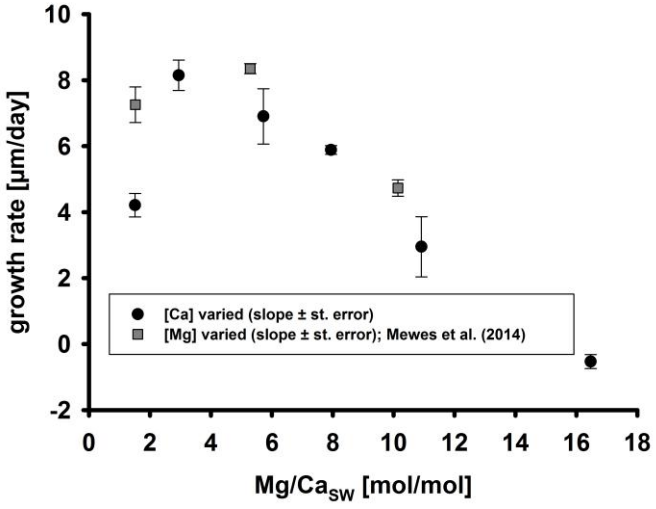

497

498 Figure 4: Growth rates [µm/day], derived from linear regression curves fitted to size data of the
499 first 30 days in culture, versus Mg/Ca_{SW}.

500

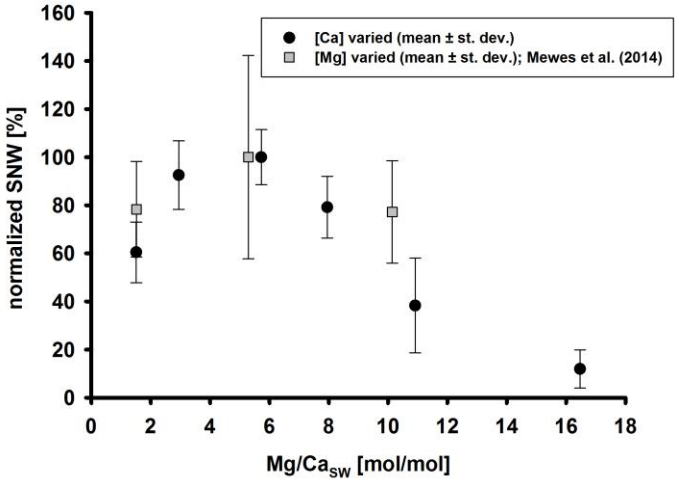

501

502 Figure 5: % mean size normalized weight [µg/µm] versus Mg/Ca$_{SW}$.

503

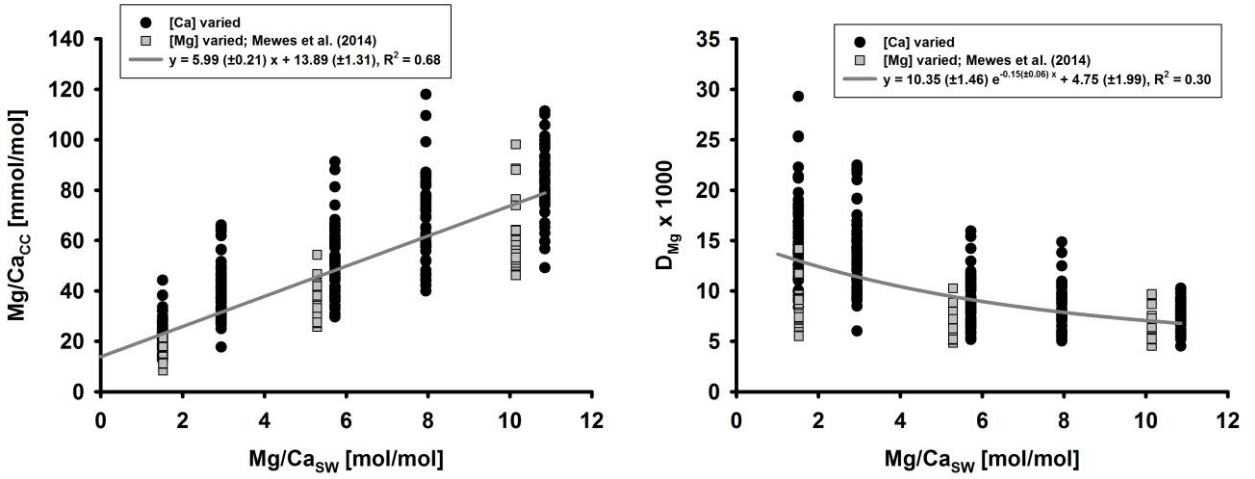

a) b)

504 Figure 6: a) Mg/Ca$_{CC}$ versus Mg/Ca$_{SW}$. b) D$_{Mg}$ x 1000 versus Mg/Ca$_{SW}$. Grey lines represent
505 functions fitted to the combined dataset.

506

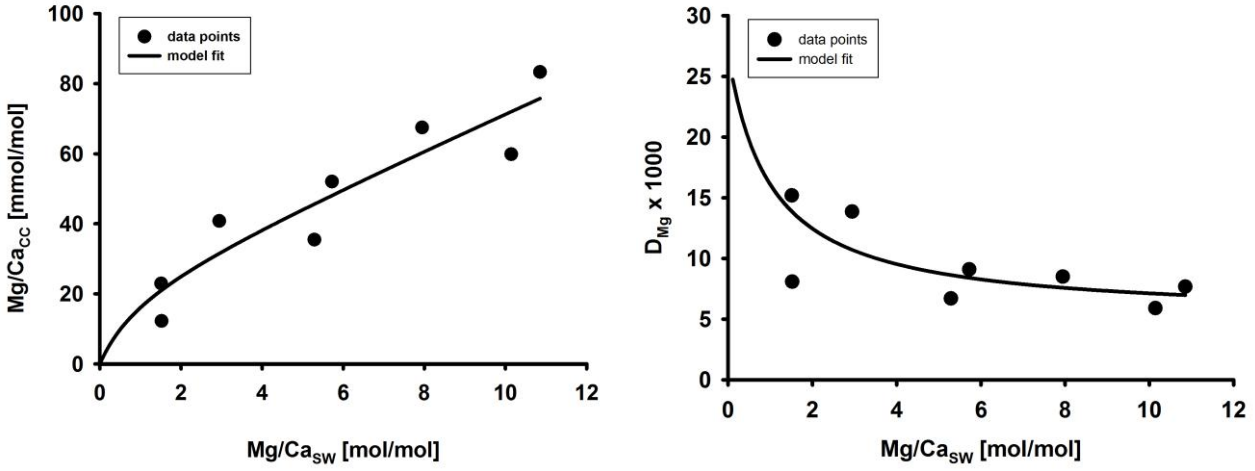

a) b)

Figure 7: Model fit to the data of our present and previous study (Mewes et al., 2014) for a) Mg/Ca_{CC} versus Mg/Ca_{SW}. b) D_{Mg} x 1000 versus Mg/Ca_{SW}.